Chinese Chemical Letters 35 (2024) 108603

Contents lists available at ScienceDirect

Chinese Chemical Letters

journal homepage: www.elsevier.com/locate/cclet

Uniform lithium deposition induced by copper phthalocyanine additive for durable lithium anode in lithium-sulfur batteries

Ting Hu, Yuxuan Guo, Yixuan Meng, Ze Zhang*, Ji Yu, Jianxin Cai, Zhenyu Yang*

Key Laboratory of Jiangxi Province for Environment and Energy Catalysis, School of Chemistry and Chemical Engineering, Nanchang University, Nanchang 330031, China

ARTICLE INFO

Article history:
Received 20 April 2023
Revised 15 May 2023
Accepted 23 May 2023
Available online 25 May 2023

Keywords:
Copper phthalocyanine
Electrolyte additive
Stable SEI film
Stabilized Li anode
Lithium-sulfur batteries

ABSTRACT

Copper phthalocyanine (CuPc) is adopted as an electrolyte additive to stabilize lithium anode for lithium-sulfur (Li-S) batteries. CuPc with a planar molecular structure and lithiophilic N-containing group, is likely to be adsorbed on the surface of Li anode to form a coating layer, which can restrict the direct contact between Li anode and solvents, and guide the uniform deposition of Li^+ ions. The Li||Li symmetric cells demonstrate a stable cycle performance, and Li||Cu cells show high Coulombic efficiencies. In Li-S batteries, the formed stable solid-electrolyte interface (SEI) film containing copper sulfides can protect Li anode from the polysulfide corrosion and side reactions with the electrolyte, leading to the compact and smooth surface morphology of Li anode. Therefore, the Li-S batteries with CuPc additive deliver much higher capacity, better cycle performance and rate capability as compared to the one without CuPc additive.

Metal Li represents one of the most perspective anode materials owing to its high theoretical capacity of 3860 mAh/g and the most negative potential of −3.04 V [1–5]. When coupled with a high-capacity sulfur cathode, the equipped Li-S battery offers a relatively high energy density of ~2600 Wh/kg, which exceeds over 3-times to that of commercial Li-ion batteries [6–10]. However, the dissolution-deposition reaction of sulfur cathode comes with a lot of problems that need to be solved. Firstly, solid sulfur converts to soluble long-chain lithium polysulfides (LiPSs) in the electrolyte, which will then cross through the separator to Li anode side, causing irreversible loss of active materials and the rapid capaicty decay [11–16]. Secondly, the reaction between Li metal and the electrolyte, and the nonuniform deposition of Li result in unstable solid electrolyte interface (SEI). The SEI continuously breaks during repeated plating/stripping process, and allows the fresh Li metal to be exposed, which is highly reactive to further react with the electrolyte [17–19]. In addition, the uncontrolled growth of Li dendrites can pierce the separator and lead to the direct connection of cathode and anode, resulting in short circuit phenomenon [20,21]. These problems eventually cause low columbic efficiency and inferior cycling stability of Li-S batteries.

To address the challenges arising on Li anode side, investigators have found several solutions, such as adopting three-dimensional current collectors [22–26], creating artificial layers of solid electrolyte [27–29], and using solid-state electrolyte with high mechanical modulus [30–34]. Compared with these strategies, modifying the electrolyte with functional additives is more simple, and these additives are helpful to *in situ* form a stable passivation film on the surface of Li anode, so as to improve its cycling lifespan [35–41]. For example, inorganic nitrates have been added into the ether-based eletrolytes to improve the Coulombic efficiency owing to the formed stable Li_xNO_y layer on Li anode surface [42,43]. Our group previously demonstrated rare-earth metal nitrates as electrolyte additives, and these nitrates showed advantages in stabilizing Li anode for Li-S batteries [44]. In addition, some organic molecules have also adoped to regulate the electrochemical deposition of Li^+ ions for dendrite-free Li anodes [45–48]. In view of the simple operation and remarkable effectiveness, the exploration of electrolyte additives is very meaningful to realize long-lasting Li anode for efficient Li-S batteries.

In this work, we have employed copper phthalocyanine (CuPc) as an additive to protect Li metal anode and thus enhance the electrochemical performance of Li-S batteries. In particular, CuPc contains lithiophilic N-functional groups, and is likely to be adsorbed on the Li anode surface, which can not only protect Li anode from the side reactions with the electrolyte, but also effectively regulate the deposition of Li^+ ions. In addition, the formed stable SEI film containing copper sulfides can effectively passivate the Li anode and suppress the continuous consumption of Li by both the solvents and LiPSs, thus benefiting for achieving the compact

* Corresponding authors.
E-mail addresses: zhangze@ncu.edu.cn (Z. Zhang), zyyang@ncu.edu.cn (Z. Yang).

https://doi.org/10.1016/j.cclet.2023.108603
1001-8417/

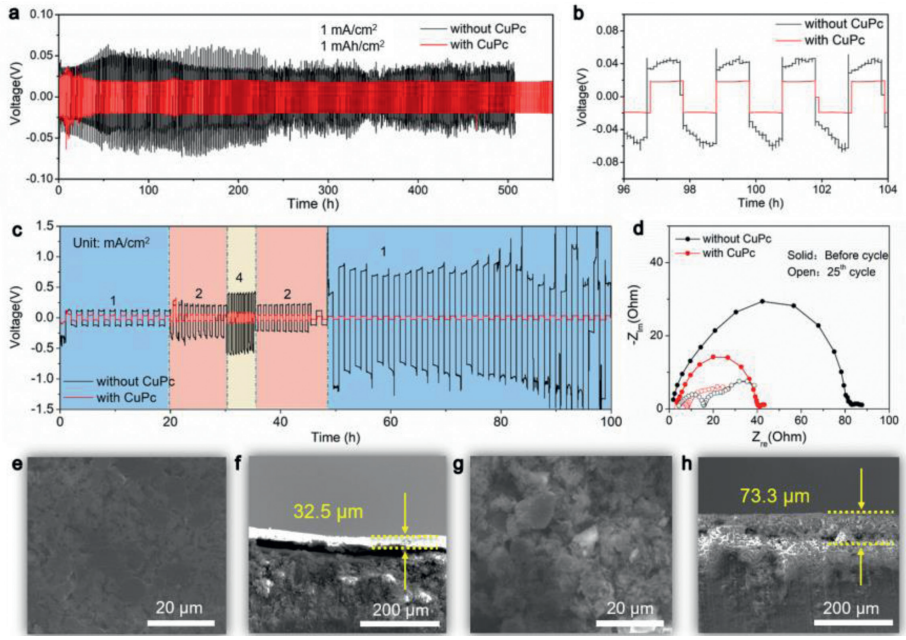

Fig. 1. Electrochemical performance of Li||Li cells. (a) Voltage profiles at 1 mA/cm^2 (1 mAh/cm^2), and (b) enlarged plots of (a). (c) Rate performance at various current densities with a fixed capacity of 1 mAh/cm^2. (d) EIS profiles of Li||Li cells before and after 25 cycles with different electrolytes at 1 mA/cm^2 (1 mAh/cm^2). Top-view and side-view SEM images of cycled Li anode (e, f) with or (g, h) without CuPc additive.

and smooth surface morphology of Li anode. With 1 mmol/L CuPc added into the electrolyte, Li||Li cells show excellent durability and Li||Cu cells show high Coulomb efficiencies. Moreover, when applied in Li-S batteries, the CuPc additive can provide a noticeable enhancement in the rate capability and stable performance.

Figs. 1a and b show the voltage distribution of Li||Li cells in the electrolytes with or without 1 mmol/L CuPc additive under a current density of 1 mA/cm^2 and a capacity of 1 mAh/cm^2. The voltage profile of the cell without CuPc additive shows obvious fluctuation and high overpotentials, which may be attributed to the exposure of Li metal caused by SEI fragmentation, and rapid uneven growth of Li dendrites. On the contrary, the cell with CuPc additive is able to achieve an excellent stability over 500 h with a low overpotential of ~20 mV. The impact of the concentrations of CuPc additive on the Li depostion behavior has also investigated. As displayed in Fig. S1 (Supporting information), at a low concentration of 0.5 mmol/L CuPc, the cell shows a steady voltage profile over 240 h, while the cell with 2 mmol/L CuPc shows obvious voltage fluctuations after about 150 h, as like the control cell withou CuPc. These results suggest that a reasonable concentration of CuPc additive is needed for better performance of Li||Li cells. In addition, Pc molecule without a metal center is also investigated as the additive for Li||Li cells. As shown in Fig. S2 (Supporting information), Pc additive can also induce steady voltage of Li||Li cell during cycling, indicating the positive role of Pc molecule in regulating Li deposition behavior. On the other hand, the overpotential value (~25 mV) of the cell with 1 mmol/L Pc is a little higher than that of the cell with 1 mmol/L CuPc, suggesting the exsitence of Cu center further contribute to the regulation of Li deposition bahavior. When tested under a higher capacity of 3 mAh/cm^2 (Fig. S3 in Supporting information), or a higher current density of 4 mA/cm^2 (Fig. S4 in Supporting information), the cells with CuPc additive deliver excellent stability with low overpotentials. The plating/stripping tests are further investigated at different current densities ranging from 1 mA/cm^2 to 4 mA/cm^2 with the capacity of 1 mAh/cm^2 (Fig. 1c). As seen, the much lower overpotentials indicate the better rate capability of the cell with CuPc additive. Fig. 1d shows electrochemical impedance spectroscopy (EIS) profiles of Li||Li cells before and after 25 cycles at 1 mA/cm^2 (1 mAh/cm^2). The impedances of the cell containing CuPc additive are much lower than that of the control cell, which proves the improved Li/electrolyte interfacial affinity and faster kinetic bahavior of Li^+ ions. In addition, the exchange current density (I_0) in Li||Li cells with CuPc additive were calculated as 1.06 mA/cm^2 from Tafel plots (Fig. S5 in Supporting information), higher than that of the cell without CuPc (0.812 mA/cm^2). This implies the better charge transfer capability across a smooth and flat surface of Li anode at the presence of CuPc. Moreover, the transfer number of Li^+ ions is assessed by using the potentiostatic polarization (Fig. S6 in Supporting information) and EIS measurements (Fig. S7 in Supporting information). The value in the cell with CuPc additive is calculated as 0.78, which is higher than that for the cell without CuPc additive (0.72). It is probably because of the complexation between Li^+ ions and the lithiophilic N elements in CuPc. As a result, CuPc molecules are likely adsorbed on Li anode surface as a coating layer, which can not only promote the Li^+ ion transfer, but also reduce the direct contact between Li anode and the solvents and inhibit the growth of dendrites. Therefore, a stable SEI film can be produced to enable excellent cycle stability of Li||Li cells.

In order to clarify the modification of Li surface morphology by CuPc additive, Scanning electron microscopy (SEM) images of Li foils disassembled from tested Li||Li cells after 100 cycles at 1 mA/cm^2 (1 mAh/cm^2). Li foil tested with CuPc additive shows a flat surface with only a few of cracks (Fig. 1e), suggesting that an uniform dissolution/deposition of Li during cycling. However, the Li foil tested without CuPc additive displays an uneven surface with severe pulverization (Fig. 1g). Such a obvious change of surface morphology suggests the uneven dissolution/deposition of Li in the basic electrolyte. Side-view SEM images (Figs. 1f and h) show the thicknesses of the surface passivation films are about 32.5 and 73.3 μm for the tested Li with or without CuPc additive, respectively. Therefore, the applied CuPc additive helps to construct a robust SEI on Li surface, and such a stable SEI can suppress the continuous consumption of both Li metal and the electrolyte.

Li||Cu cells were further applied to evoluate the Coulombic efficiency (CE) and Li anode. As shown in Fig. 2a, with the presence

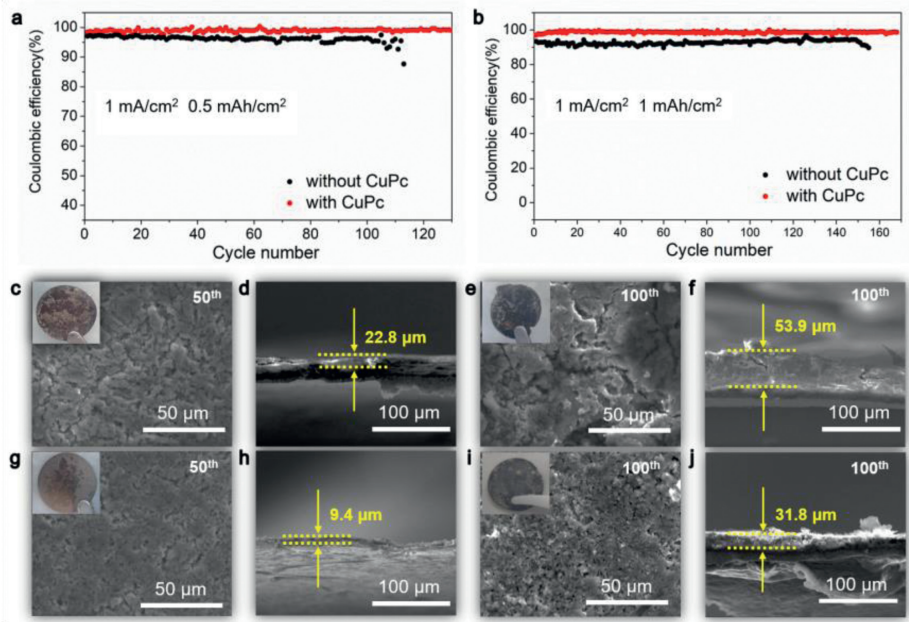

Fig. 2. Coulombic efficiency of Li||Cu cells at a current density of 1 mA/cm^2 and the capacity of (a) 0.5 mAh/cm^2 and (b) 1 mAh/cm^2. Top-view and side-view SEM images of Li deposited onto Cu foils after different cycles at 1 mA/cm^2 (1 mAh/cm^2) in the electrolyte (c-f) without or (g-j) with CuPc. The insets show the digital images of deposited Li on Cu foils.

of CuPc additive, the Li||Cu cell shows a high initial CE of ~99% compared with that of the control cell (~97%). However, after 113 cycles, the control cell shows a rapidly falling charge capacity, leading to the decreased CE to 87.6%. While the cell with CuPc additive shows stable voltage profiles and higher CE. At a high deposition capacity, the cell with CuPc additive also shows higher CE compared with the one without CuPc (Fig. 2b). The deposition behaviors of Li on Cu foil were investigated by SEM. The tested Cu foils were disassembled from the Li||Cu cells after cycled at 1 mA/cm^2 (1 mAh/cm^2). In the basic electrolyte, the deposited Li on the Cu foil surface shows a loose and cracked morphology, which becomes more uncontrolled and irregular along with the increasing cycles (Figs. 2c and e). For the modified electrolyte, the deposited Li exhibits a relatively dense and flat morphology (Figs. 2g and i). The side-view SEM images demonstrate the thinner deposited layer at the presence of CuPc (Figs. 2h and j) in comparsion with the basic electrolyte (Figs. 2d and f). This means that CuPc additive can effectively homogenize the deposition of Li and help to form a stable SEI film, thereby greatly restraining the growth of dendrites.

Fig. 3a displays the rate performance of Li-S batteries with or without CuPc additive. The battery with CuPc additive delivers an initial specific capacity of 1146 mAh/g at 0.1 C, and shows much higher capacities at higher C rates. Even at 4 C, a high discharge capacity of 560 mAh/g is realized, which largely exceeds that of the cell without CuPc additive (~200 mAh/g). It is known that the uncontrolled shuttle effect can not only lead to the irreversible loss of sulfur active materials, but also the rapid degradation of Li anode due to the continuous deposition of insulating Li_2S_2/Li_2S layer. This further leads to the capacity decay especially at high C rates due to the increasing polarization. As reflected in the discharge/charge curves (Fig. S8 in Supporting information), the battery without CuPc additive shows huge polarization and severe shrinkage of the discharge plateau, especially the second one that contributes the majority of cathode capacity. While the battery with CuPc additive shows typical two-step potential plateau (Fig. 3b) and smaller polarization values between the charge and discharge potential plateaus (Fig. 3c) at various C rates, indicating the better rate capability of Li-S batteries. In additive, the cyclic voltammetry (CV) profiles are compared in Fig. S9 (Supporting information), and the cell with CuPc additive shows a lower potential polarization between cathodic peak and anodic peak. This reveals the better reversibility of sulfur redox reactions by the catalysis effect of CuPc additive, as reported for CoPc [49,50], FePc [51], and other metal-based Pc [52]. The effect of the concentration of CuPc additive on the battery performance has been investigated. Compared with the basic electrolyte, the modified electrolytes with different concentrations of CuPc additive (0.5 mmol/L and 2 mmol/L) come with the improved rate performance of Li-S batteries (Fig. S10 in Supporting information). The two-step potential plateau of the sulfur cathodes maintains well along with the increasing C rates (Fig. S11 in Supporting information). Besides, an optimal concentration of CuPc additive (1 mmol/L) is necessary for best electrochemical performance. This should be related to the wettability of different electrolytes. As shown in Fig. S12 (Supporting information), the introduction of CuPc improve the wettability of the eletrolyte on the separator surface with lower contact angles. In addition, with 1 mmol/L CuPc additive, the lowest contact angle of 30.5° is obtained. Smaller contact angle implies better wettability of the electrolyte, which enables better interfacial compatibility and accelerates the Li^+ ion diffusion.

In Fig. 3d, the battery with CuPc additive shows a high initial capacity of 825.6 mAh/g at 0.5 C, and maintains at 677.8 mAh/g after 150 cycles. The capacity fading rate is about 0.12% per cycle. As a comparsion, the capacites of the battery without CuPc rapid decrease from 700.3 mAh/g to 516.7 mAh/g, suggesting a high fading rate of 0.17% per cycle. Moreover, CuPc additive enables higher average CE (~99%). The superiority of CuPc additive maintains even cycling at 1 C, supported by the better stability of Li-S battery. In order to further evaluate the advantage of CuPc additive, the cycling performances of high-loading sulfur cathodes (~3 mg/cm^2) were evaluated. Fig. 3e shows that the specific capacities are 872.1 and 602.4 mAh/g at the 1st cycle, and keep at 698.3 and 552.1 mAh/g at the 50th cycle with the E/S ratios of 9 and 7 μL/mg, respectively. The capacity retentions are about 80.1% and 91.6%, respectively, implying the good stability. The maintained two discharge potential plateaus (Fig. 3f) at such harsh operat-

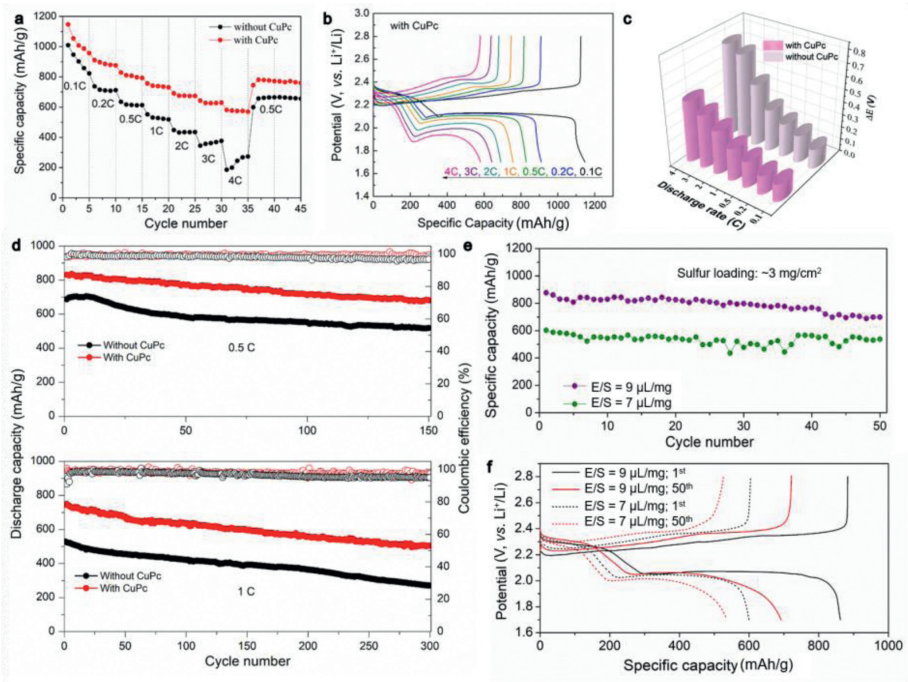

Fig. 3. (a) Rate performance of Li-S batteries with or without CuPc additive. (b) Galvanostatic discharge-charge curves of Li-S cells with CuPc additive at different current densities (1 C=1675 mA/g). (c) Polarization potential at various rates. (d) Cycle performance of Li-S cell with CuPc additive at 0.5 C and 1 C. (e) Cycle performance and (f) glvanostatic discharge-charge curves of Li-S cell with CuPc additive with high-loading sulfur cathodes at 0.1 C.

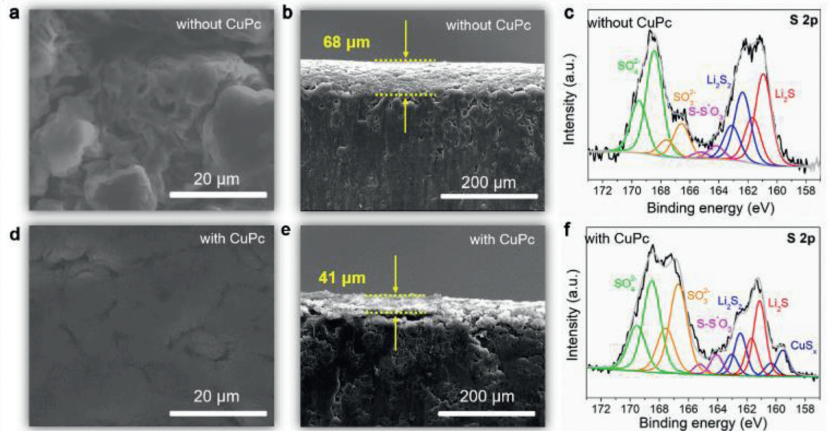

Fig. 4. Top-view and side-view SEM images of Li anode surface (a, b) without and (d, e) with CuPc additive after cycled at 0.5 C. S 2p spectra of the cycled Li anode (c) without and (f) with CuPc additive.

ing conditions suggests the good kinetics of sulfur redox reactions enabled by CuPc additive. As control, the batteries without CuPc show lower specific capcities and faster capacity decay at the same condition (Fig. S13 in Supporting information). These results definitely demonstrate the positive role of CuPc additive in improving the electrochemical performance of sulfur cathodes.

The morphologies of cycled Li anode were observed by SEM. In the case of the electrolyte without CuPc additive, the cycled Li exhibits a cracked and loose surface morphology (Fig. 4a), implying that the formed SEI is fragile during the long-term cycling. This will do harm to the cycle stability of both Li anode and sulfur cathode. However, the Li anode cycled in the electrolyte with CuPc additive owns relatively compact and smooth surface (Fig. 4d). This further verifies the positive role of CuPc on forming a stable SEI on Li surface. In the basic electrolyte, Li dendrites are more likely to be generated due to the uneven SEI formation. It will cause more serious damage corrosion to Li anode. The thickness of the passivation layer on the surface of cycled Li anode cycled is as high as ~68 μm (Fig. 4b). While the thickness of the passivation layer is only ~41 μm for the Li anode cycled with CuPc additive (Fig. 4e). It can be seen that after adding CuPc additive to the basic electrolyte, the N functional group in CuPc can effectively regulate lithium ion deposition. X-ray photoelectron spectroscopy (XPS) was further carried out to determine the composition of different SEI films. As presented in Fig. 4c, S 2p spectra shows two obvious peaks for the Li anode cycled in the basic electrolyte. The peak in the low-energy region can be divided to three components including Li_2S (160.9 eV), Li_2S_2 (162.3 eV), and S-S*O_3 (164.2 eV), while the one in the high-energy region can be assigned to SO_x^{2-} groups [53,54]. With the addition of CuPc (Fig. 4f), an extra peak appears at the binding energy of 159.5 eV, which suggests the formation of copper sulfide species. The formed SEI is not susceptible to fragmentation, and is conducive for protecting Li anode from the continuous corrosion by both soluble LiPSs and the sol-

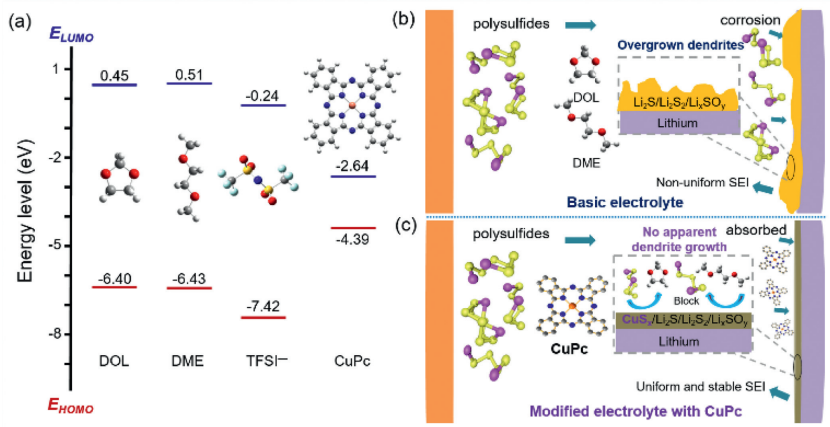

Fig. 5. (a) The molecular orbitals and energies for the HOMO and LUMO of CuPc, DOL, DME and TFSI⁻ (gray: carbon. White: hydrogen. Red: oxygen. Blue: nitrogen. Orange: copper. Yellow: sulfur. Pink: lithium). Schematic illustration of the deposition behaviors of Li (b) without and (c) with CuPc additive.

vents [55]. As a result, the irreversible deposition of Li_2S_2/Li_2S on the anode surface is greatly suppressed, which can be identified by the reduced area ratio of Li_2S_2/Li_2S. Moreover, according to the C 1s spectra (Fig. S14 in Supporting information), the peak at 283.3, 285.9, 286.3 and 287.3 eV, can be corresponded to the characteristic peaks of C–C bond in CuPc, shake-up transition of CuPc, C–H and C–N bond, respectively [56]. Besides, as displayed in the Cu 2p spectra (Fig. S15 in Supporting information), Cu $2p_{1/2}$ and Cu $2p_{3/2}$ peaks at 952.7 and 933.2 eV, respectively [56]. Therefore, it can be concluded from the above discussion that CuPc participates in the formation of stable SEI on Li surface, and the formed SEI plays a positive role in stabilizing Li metal.

The density function theory (DFT) calculation was conducted to reveal the highest occupied molecular orbital/lowest unoccupied molecular orbital (HOMO/LUMO) of CuPc, solvents (DOL, DME) and TFSI⁻. As shown in Fig. 5a, the energies of LUMO levels of CuPc, DOL, DME and TFSI⁻ are calculated as 0.45, 0.51, −0.24 and 2.64 eV, while the HOMO levels are −6.40, −6.43, −7.42 and −4.39 eV, respectively. Obviously, CuPc has the lowest LUMO level, indicating more favorable reduction of CuPc during the electrochemical cycling. In other words, Li anode cycled in the basic electrolyte is easily damaged by the unwanted side reactions with the solvents and TFSI⁻anion, as well as soluble LiPSs (Fig. 5b), leading to the overgrown dendrites and nonuniform SEI. However, in the modified electrolyte (Fig. 5c), CuPc is more easily to participate in the formation of stable SEI film on the Li anode surface, thereby proctecting Li anode from the side reactions with the electrolyte, suppressing the dendrite formation and reducing the polysulfide corrosion of Li anode. Thus, the cycle stabilities of both Li anode and sulfur cathode are significantly enhanced by CuPc additive.

In summary, we have reported CuPc as an electrolyte additive to stabilize Li anode for Li-S batteries. CuPc additive is likely to be adsorbed on Li anode surface as a functional molecule-level coating layer, which helps to regulate the depotion behaviors of Li, reduce the direct contact between Li anode the electrolyte, and suppress the growth of Li dendrites. Li||Li cells with CuPc additive show excellent cycle stability with low overpotentials and outstanding rate performance. Meanwhile, in the case of Li-S batteries, the formed stable SEI film containing copper sulfides can effectively restrict the continuous deposition of Li_2S_2/Li_2S on Li anode surface, which can not only suppress the formation of dead sulfur, but also protect Li anode from the contiunous corrosion of soluble LiPSs. Thus, the Li-S batteries with CuPc additive deliver much higher capacity, better cycle performance and rate capability. This work provides a new and simple way to improve the stability of metal Li anode for Li-S batteries and other advanced rechargeable Li metal batteries.

Declaration of competing interest

The authors declare no competing financial interests or personal relationships that could have appeared to influence the work reported in this paper.

Acknowledgments

This work is supported by the National Natural Science Foundation of China (NSFC, Nos. 22269013, 22263009), the Natural Science Foundation of Jiangxi Province (Nos. 20224ACB213001, 20202ACB202004, 20213BCJ22024, 20212BBE53051), and the Key Laboratory of Jiangxi Province for Environment and Energy Catalysis (No. 20181BCD40004).

Supplementary materials

Supplementary material associated with this article can be found, in the online version, at doi:10.1016/j.cclet.2023.108603.

References

[1] G.X. Lu, J.W. Nai, D.Y. Luan, et al., Sci. Adv. 9 (2023) eadf1550.
[2] J.C. Cui, T.G. Zhan, K.D. Zhang, D. Chen, Chin. Chem. Lett. 28 (2017) 2171–2179.
[3] S.S. Qian, H. Chen, M.T. Zheng, et al., Energy Storage Mater. 57 (2023) 229–248.
[4] L.Y. Tian, Z. Zhang, S. Liu, G.R. Li, X.P. Gao, Nano Energy 106 (2023) 108037.
[5] X.Z. Fan, M. Liu, R.Q. Zhang, et al., Chin. Chem. Lett. 33 (2022) 4421–4427.
[6] C. Xing, Chen H, S.S. Qian, et al., Chem 8 (2022) 1201–1230.
[7] M. Nojabaee, B. Sievert, M. Schwan, et al., J. Mater. Chem. A 9 (2021) 6508–6519.
[8] T. Yang, K. Liu, T. Wu, et al., J. Mater. Chem. A 8 (2020) 18032–18042.
[9] F. Li, L. Wang, G.M. Qu, et al., Chin. Chem. Lett. 33 (2022) 3909–3915.
[10] Q.B. Liu, Y.J. Wu, D. Li, et al., Adv. Mater. 35 (2023) 2209233.
[11] M. Rana, S.A. Ahad, M. Li, et al., Energy Storage Mater. 18 (2019) 289–310.
[12] J. Lei, T. Liu, J. Chen, et al., Chem 6 (2020) 2533–2557.
[13] R. Fang, K. Chen, L. Yin, et al., Adv. Mater. 31 (2019) 1800863.
[14] Z. Shi, M. Li, J. Sun, Z. Chen, Adv. Energy Mater. 11 (2021) 2100332.
[15] X.Y. Liu, H.J. Peng, B.Q. Li, et al., Angew. Chem. Int. Ed. 61 (2022) e202214037.
[16] J.K. Hu, H. Yuan, S.J. Yang, et al., J. Energy Chem. 71 (2022) 612–618.
[17] Z.X. Chen, L.P. Hou, C.X. Bi, Q. Cheng, X.Q. Zhang, Energy Storage Mater. 53 (2022) 315–321.
[18] C. Yan, R. Xu, Y. Xiao, et al., Adv. Funct. Mater. 30 (2020) 1909887.
[19] K. Hankins, V. Prabhakaran, S. Wi, et al., J. Phys. Chem. Lett. 12 (2021) 9360–9367.
[20] T. Tao, S. Lu, Y. Fan, et al., Adv. Mater. 29 (2017) 1700542.
[21] H. Duan, Y.X. Yin, Y. Shi, et al., J. Am. Chem. Soc. 140 (2018) 82–85.
[22] Y. Du, X. Gao, S.W. Li, L. Wang, B. Wang, Chin. Chem. Lett. 31 (2020) 609–616.
[23] Q. Yun, Y.B. He, W. Lv, et al., Adv. Mater. 28 (2016) 6932–6939.
[24] R. Zhang, X. Chen, X. Shen, et al., Joule 2 (2018) 764–777.
[25] T.Y. Zhou, Y.L. Mu, J.Y. Wu, et al., Chin. Chem. Lett. 33 (2022) 2165–2170.

[26] X. Han, T.T. Wu, L.H. Gu, et al., Chin. Chem. Lett. 34 (2023) 107594.
[27] J. You, H. Deng, X. Zheng, et al., ACS Appl. Mater. Interfaces 14 (2022) 5298–5307.
[28] C. Zou, L. Yang, K. Luo, et al., ACS Appl. Energy Mater. 5 (2022) 8428–8436.
[29] S.K. Huo, Y.F. Zhang, Y. He, et al., J. Phys. Chem. Lett. 14 (2023) 16–23.
[30] S.Y. Zhou, S.J. Zhong, Y.F. Dong, et al., Adv. Funct. Mater. 33 (2023) 2214432.
[31] X.Y. Meng, Y.Z. Liu, Y.F. Ma, et al., Adv. Mater. 35 (2023) 2212039.
[32] B. Ding, J. Wang, Z.J. Fan, et al., Mater. Today 40 (2020) 114–131.
[33] Q.J. Yu, K.C. Jiang, C.L. Yu, et al., Chin. Chem. Lett. 32 (2021) 2659–2678.
[34] J. Liu, H. Yuan, H. Liu, et al., Adv. Energy Mater. 12 (2022) 2100748.
[35] S. Xia, X. Zhang, C. Liang, Y. Yu, W. Liu, Energy Storage Mater. 24 (2020) 329–335.
[36] F.Y. Liu, C.X. Zong, L. He, et al., Chem. Eng. J. 443 (2022) 136489.
[37] N. Zhong, C.J. Lie, R.J. Meng, et al., Small 28 (2022) 2200046.
[38] B.Q. Wang, S.H. Lu, P.Y. Zhang, et al., Energy Technol. 11 (2023) 2201110.
[39] S. Kim, Y.M. Kwon, K.Y. Cho, S. Yoon, Electrochim. Acta 391 (2021) 138927.
[40] S.J. Zhang, B. Cheng, Y.X. Fang, et al., Chin. Chem. Lett. 33 (2022) 3951–3954.
[41] X.H. Hu, J.D. Liu, Y.X. Yang, et al., Chin. Chem. Lett. 34 (2023) 108456.
[42] J. Tan, M.X. Ye, J.F. Shen, Mater. Horiz. 9 (2022) 2325–2334.
[43] S. Liu, G.R. Li, X.P. Gao, ACS Appl. Mater. Interfaces 8 (2016) 7783–7789.
[44] M.Z. Huang, T. Hu, Y.T. Zhang, et al., ACS Appl. Mater. Interfaces 14 (2022) 17959–17967.
[45] L. Xu, J. Yang, M. Huang, et al., Chem. Eng. J. 419 (2021) 129494.
[46] Z. Xie, Z. Wu, X. An, et al., Chem. Eng. J. 393 (2020) 124789.
[47] F. Liu, C. Zong, L. He, et al., Chem. Eng. J. 443 (2022) 136489.
[48] J.P. Sun, K. Zhang, Y.Z. Fu, W. Guo, Nano Res. 16 (2023) 3814–3822.
[49] W.L. Huang, Z.J. Lin, H.T. Liu, et al., J. Mater. Chem. A 6 (2018) 17132–17141.
[50] X.X. Yang, X.T. Li, C.F. Zhao, et al., ACS Appl. Mater. Interfaces 12 (2020) 32752–32763.
[51] S. Zhuo, S. Yang, X.W. Ding, et al., ACS Nano 14 (2020) 7538–7551.
[52] X.D. Song, F.Y. Zhou, M. Yao, C. Hao, J.S. Qiu, ACS Sustain. Chem. Eng. 8 (2020) 10185–10192.
[53] Y. Wang, L.F. Zhu, J.X. Wang, et al., Chem. Eng. J. 433 (2022) 133792.
[54] F.J. Liu, Y.T. Zhu, L.Q. Liu, et al., Inorg. Chem. 62 (2023) 5219–5228.
[55] H. Dai, J. Dong, M. Wu, et al., Angew. Chem. Int. Ed. 60 (2021) 19852–19859.
[56] D. Lee, S. Sun, J. Kwon, et al., Adv. Mater. 32 (2020) 1905573.